

**Purdue University**  
**Purdue e-Pubs**

---

International Refrigeration and Air Conditioning  
Conference

School of Mechanical Engineering

---

2004

# Scroll Expander for Carbon Dioxide Air Conditioning Cycles

Detlef Westphalen  
*TIAX LLC*

John Dieckmann  
*TIAX LLC*

Follow this and additional works at: <http://docs.lib.purdue.edu/iracc>

---

Westphalen, Detlef and Dieckmann, John, "Scroll Expander for Carbon Dioxide Air Conditioning Cycles" (2004). *International Refrigeration and Air Conditioning Conference*. Paper 690.  
<http://docs.lib.purdue.edu/iracc/690>

This document has been made available through Purdue e-Pubs, a service of the Purdue University Libraries. Please contact [epubs@purdue.edu](mailto:epubs@purdue.edu) for additional information.

Complete proceedings may be acquired in print and on CD-ROM directly from the Ray W. Herrick Laboratories at <https://engineering.purdue.edu/Herrick/Events/orderlit.html>

## SCROLL EXPANDER FOR CARBON DIOXIDE AIR CONDITIONING CYCLES

**Detlef Westphalen<sup>1</sup>, John Dieckmann<sup>2</sup>**

TIAX LLC; 15 Acorn Park, Cambridge, MA 02140, USA

<sup>1</sup>Tel.: 617-498-5821; Fax: 617-498-7213; E-Mail: Westphalen.D@Tiaxllc.com

<sup>2</sup>Tel.: 617-498-5818; Fax: 617-498-7213; E-Mail: Dieckmann.J@Tiaxllc.com

### ABSTRACT

A scroll expander design has been developed for use in carbon dioxide air-conditioning cycles operating in high ambient conditions. The expander efficiency is projected to be 70% based on design study and analysis. Cycle analysis, used to establish expander operating conditions, indicates that system power input will be reduced about 20% for a system using a 60%-efficient expander. Analysis shows that the most attractive approach for utilization of expander shaft power is to use it to offset compressor shaft power in an integrated compressor/expander unit.

### 3. INTRODUCTION

The use of CO<sub>2</sub> as a refrigerant has been receiving attention recently because it is a “natural” refrigerant which is not flammable or toxic. Furthermore, it is inexpensive, widely available worldwide from numerous suppliers, and not subject to venting restrictions. The major challenge is to design a cost-effective, efficient system that accommodates the unique characteristics of CO<sub>2</sub>, which differ from those of fluorocarbon refrigerants.

Both theoretical and experimental studies have concluded that the thermodynamic cycle efficiency of transcritical CO<sub>2</sub> systems is lower than that of conventional fluorocarbon-based vapor compression systems, particularly at high ambient temperatures. A decrease in system efficiency could negate part or all of the environmental advantage of the CO<sub>2</sub> system by increasing its indirect contribution to global warming due to the higher energy consumption. Furthermore, it would be unacceptable in either military or commercial markets to introduce systems with lower efficiencies than existing units. An approach to improving the efficiency of transcritical CO<sub>2</sub> systems must be found in order to spur commercialization. Fortunately, such an opportunity exists in recovering the large losses that occur during the expansion process of the refrigerant between the exit of the high-pressure gas cooler and the evaporator.

In theory, recovery of energy lost in the expansion process of a vapor compression cycle is of interest for any refrigerant. However, due to the large losses of expansion of CO<sub>2</sub>, attributable to the high operating pressures, a work recovery device is particularly important [see, for example, Heidelck and Kruse (2000), Robinson and Groll (1998)]. The work described in this paper addresses development of an energy recovery scroll expander design for use in a military environmental control unit (ECU).

The U.S. Army has developed and fielded a family of electronic shelter ECUs, ranging in capacity from 6,000 Btu/hr [1.8 kW] to 60,000 Btu/hr [17.6 kW]. There are currently about 20,000 of these ECUs under deployment or in inventory. Expanding use of electronic equipment on the battlefield will lead to procurement of more ECUs in the future, especially in the larger capacity sizes. The expander design described in this paper is based on application of CO<sub>2</sub> air-conditioning technology to a 36,000 Btu/hr [10.5 kW] horizontal ECU. The performance and physical specifications of current and future Improved ECUs (IECUs) for this unit are shown in Table 1 below. The IECU program, based on use of HFC refrigerants, is currently in development phases and is not in production.

The U.S. Army's interest in ECUs using CO<sub>2</sub> refrigerant is based on the following anticipated benefits.

- Elimination of logistics costs for equipment, procedures, and training associated with refrigerant recovery, which is required for the HCFC and/or HFC refrigerants used with the current ECU and planned for the IECU. CO<sub>2</sub> does not require recovery, since it can be vented.
- Potential for reduction in size and weight of refrigeration circuit components.
- Reduced impact on environment, since CO<sub>2</sub> has net zero Global Warming Potential, assuming there is no efficiency penalty associated with the change in refrigerant.

**Table 1: Performance Specifications for 36,000 Btu/hr [10.5 kW] Horizontal ECUs**

	Current ECU	IECU
Operating Temperature Range for Cooling (°F [C])	Up to 120 [48.9]	-25 to 125 [-31.7 to 51.7]
Cooling Capacity Total (Btu/hr [kW])	41,000 [12.0]	36,000 [10.5]
Capacity Rating Conditions—Ambient Temp (°F [C])	120 [48.9]	125 [51.7]
Evaporator Return Air Dry Bulb/Wet Bulb (°F [C])	90 / 75 [32.2 / 23.9]	90 / 75 [32.2 / 23.9]
Maximum Power Input (kW)	13.5	10.0
Maximum Weight (lb [kg])	435 [198]	395 [180]
Max Dimensions (in [mm]) Width x Height x Depth	38 x 27 x 35	965 x 686 x 889

References 3, 4

## 2. CYCLE ANALYSIS

Cycle analysis was carried out in order to determine the design operating conditions for the expander, to optimize the design parameters, to determine the impact of the expander on the system design, and to assess operating characteristics for off-design conditions.

Key assumptions made for the cycle analysis are as follows.

- Net capacity of 36,000 Btu/hr [10.5 kW] for ambient temperature of 125 °F [51.7 C] and evaporator return conditions of 90 °F [32.2 C] dry bulb / 75 °F [23.9 C] wet bulb temperatures.
- Evaporator capacity of 39,000Btu/hr [11.4 kW] to allow for evaporator blower/motor heat and losses.
- Evaporating temperature of 55 °F [12.8 C], with 5 °F [2.8 C] evaporator exit superheat.
- Maximum compressor discharge temperature close to 270 °F [132 C].
- Gas Cooler exit temperature of 130 °F and 135 °F [54.4 and 57.2 C] (approach to ambient of 5 °F and 10 °F [2.8 and 5.6 C]).
- Use of a suction line heat exchanger (SLHX) was considered for systems with and without an expander.
- Efficiencies of 75% for the compressor, 60% and 70% for the expander, and up to 75% for the SLHX.

System performance for a range of system high pressures is summarized in Table 2 and plotted in Figure 1 for systems with and without a SLHX for operation with 135 °F [57.2 C] gas cooler exit temperature.

**Table 2: Carbon Dioxide System with Expander**

High Pressure (psia [bar])		1,700 [117]	1,800 [124]	1,900 [131]	2,000 [138]	2,100 [145]	2,200 [152]	2,300 [159]
Evaporator Δh (Btu/lb [kJ/kg])	System with SLHX	46.7 [109]	51.1 [119]	52.2 [122]	53.8 [125]	54.5 [127]	Not Calc- ulated	55.0 [128]
Mass Flow (lb/hr [kg/hr])		836 [380]	764 [347]	748 [340]	725 [330]	715 [325]		709 [322]
Exp. Inlet Vol. Flow (cfm [cc/s])		0.37 [0.10]	0.31 [0.085]	0.30 [0.082]	0.28 [0.077]	0.27 [0.074]		0.26 [0.071]
Evaporator Δh (Btu/lb [kJ/kg])	System without SLHX	26.7 [62]	32.1 [75]	36.4 [85]	39.7 [92]	42.3 [98]	44.5 [104]	46.3 [108]
Mass Flow (lb/hr [kg/hr])		1,460 [664]	1,216 [523]	1,072 [487]	982 [446]	921 [419]	876 [398]	843 [383]
Exp. Inlet Vol. Flow (cfm [cc/s])		0.87 [0.238]	0.65 [0.178]	0.52 [0.142]	0.45 [0.123]	0.40 [0.109]	0.37 [0.101]	0.34 [0.093]

Note: These results are for operation with 135 °F [57.2 C] gas cooler exit temperature

Some differences are apparent for the system without a SLHX as compared to the system with a SLHX:

- Mass flows are significantly higher for the system without SLHX in order to achieve the desired capacities.
- Expander power output is nearly doubled. This is due to the increased mass flow and the increased temperature of the expander inlet flow.
- The optimum high pressure is higher—in the range of 2,000 to 2,100psia [138 to 145 bar]. However, there is little difference in the power input for a fairly wide pressure range from 1,900 to 2,300psia [131 to 159 bar].
- Net COP is identical to that of the system without SLHX.

- Expander inlet volume flow is about 50% higher.

For the system with a SLHX, optimum high pressure is 1,900 psia [131 bar] and expander inlet volume flow is 0.3 cfm [0.082 cc/s], while for the system without a SLHX, the design high pressure would be selected as 2,000 psia [138 bar] and the volume flow would be 0.45 cfm [0.123 cc/s].

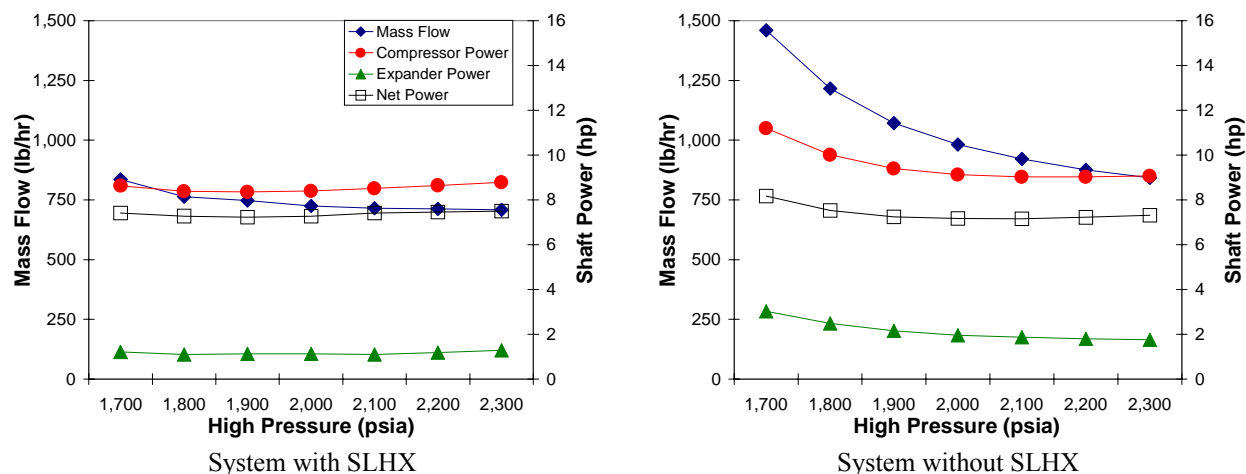


**Figure 1: ECU Design-Point Mass Flow and Compressor/Expander Power**

The isentropic expansion process represented in a pressure/volume plot for the expander for a system operating with a SLHX at 1,900 psia [131 bar] high pressure and with 135 °F [57.2 C] gas cooler exit temperature is shown in Figure 2. A large portion of the expander work output is associated with intake flow work.

A conservative assumption of 10 °F [5.6 C] approach to ambient in the gas cooler was made for initial analysis. However, approach temperatures down to 5 °F [2.8 C] are reasonable. Analysis results summarized in Table 3 show that system efficiency improves considerably for the lower approach temperature. The improvement is greater for the system without a SLHX.

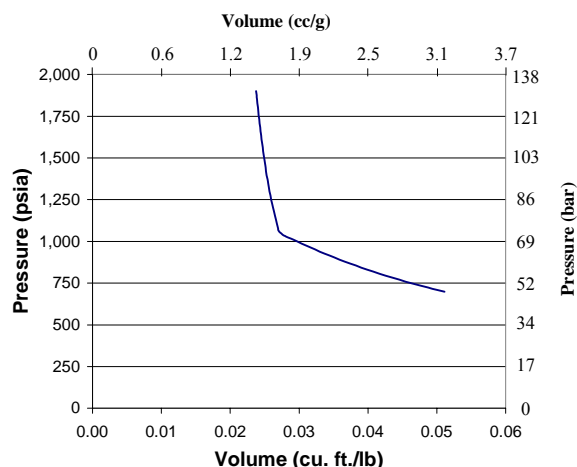


**Figure 2: Transcritical Expansion Process Pressure-Volume Diagram**

**Table 3: Impact of Gas Cooler Effectiveness**

SLHX	YES		NO	
High Pressure (psia [bar])	1,900 [131]		2,000 [138]	
GC Exit/Ambient Approach (°F [C])	10 [5.6]	5 [2.8]	10 [5.6]	5 [2.8]
Evaporator $\Delta h$ (Btu/lb [kJ/kg])	52.2 [122]	56.0 [131]	39.7 [93]	43.9 [103]
Mass Flow (lb/hr [kg/hr])	748 [340]	696 [316]	982 [446]	888 [404]
Exp. Inlet Vol. Flow (cfm [cc/s])	0.30 [0.082]	0.26 [0.071]	0.45 [0.123]	0.41 [0.112]
Shaft Power (hp [kW]): Compressor	8.4 [6.3]	7.7 [5.7]	9.1 [6.8]	8.3 [6.2]
Expander	-1.1 [-0.8]	-1.0 [-0.7]	-2.0 [-1.5]	-1.6 [-1.2]
Net	7.2 [5.4]	6.7 [5.0]	7.2 [5.4]	6.6 [4.9]
Shaft Power Reduction (%)	--	7%	--	8%

Estimates of air-conditioning system power input for systems based on CO<sub>2</sub> refrigerant (with and without an expander) and a system using HFC refrigerant are compared in Table 4 below. Information sources and key

assumptions are listed under the table. The results clearly indicate that the expander is required in order to achieve system power parity with an HFC-based system for this extreme scenario of operation in 125 °F [51.7 °C] ambient. The system efficiency improvement of utilizing the expander is 20% or more.

**Table 4: CO<sub>2</sub> Air-Conditioning System Power Input Comparison**

		Electric Power (kW)			
		Compressor/ Expander	Evaporator Blower	Gas Cooler or Condenser Blower	TOTAL
HFC-based refrigerant system		4.4	0.6	1.5	6.5
10F Gas-Cooler Approach	CO <sub>2</sub> System without expander, with SLHX	7.6	0.6	0.5	8.7
	CO <sub>2</sub> System with 60% expander	6.0	0.6	0.5	7.1
5F Gas-Cooler Approach	CO <sub>2</sub> System without expander, with SLHX	7.0	0.6	0.7	8.3
	CO <sub>2</sub> System with 72% expander	5.1	0.6	0.7	6.4

Notes: 1. HFC data based on mockup system test results. CO<sub>2</sub> data based on calculations.

2. Evaporator blower shaft power 0.7 hp [0.52 kW], motor efficiency 86%.

3. Condenser blower shaft power 1.75 hp [1.3 kW], motor efficiency 86%. Blower performance based on mockup system test results: 2,900 cfm [1.4 m<sup>3</sup>/s] at 1.6 in wc [400 Pa], blower efficiency 40%.

4. For 10° F [5.6 °C] gas cooler approach (difference between gas cooler exit temperature and ambient), gas cooler air flow 1,100 cfm [0.52 m<sup>3</sup>/s] (temperature rise up to roughly 180 °F [82 °C]) at 1.2 in wc [300 Pa], blower efficiency 40%, motor efficiency 86%. Increased gas cooler fan power for 5° F [2.8 °C] approach.

5. CO<sub>2</sub> system with expander calculation based on use of expander power for compression.

### 3. SCROLL EXPANDER DESIGN

A pair of scrolls was designed based on the expander design operating conditions. The design was based on a system utilizing a SLHX, but would be adaptable to a non-SLHX system with some dimensional adjustments. Operating conditions are as indicated by the 1,900 psia [131 bar] column of Table 2 for the SLHX system. Key design details are as follows.

- Machine speed: 3,500 rpm
- Displacement: 0.11 cu in [1.8 cc]
- Volume Ratio: 2.5
- Scroll flank Outer Diameter: 2.2" [56 mm]

While the scroll dimensions are certainly larger than a needle valve, which would be used for pressure reduction in a system without an expander, the size of the scrolls is quite modest.

Key aspects of the scroll design are as follows.

- The scroll has nearly three wraps in order to eliminate leakage directly from the inlet to the exit. Instead, refrigerant leaking through the device is caught in a downstream pocket. This allows some energy recovery from the leaked refrigerant.
- A small orbit radius was chosen to reduce sliding friction. The tradeoff for reduction in orbit radius is increased scroll tangential force and bearing loads. An orbit radius was chosen to balance these trends.
- Short wall height is selected to assure good stiffness.
- The wall thickness was a tradeoff between leakage, which increases for thinner wall thickness, and scroll disk size, which grows as the wall thickness increases.
- The flank and tip gap is intended to average 0.0003 inches [8 µm], which requires a machining tolerance of 0.0003 inches [8 µm] on all scroll surfaces. This tolerance is achievable with modern CNC machining, but is a reasonable limit for maintaining acceptable costs.

A scroll machine configuration has been developed which will allow for efficient transfer for the scroll output power to a rotating shaft. Key features of this design configuration are as follows.

- Leakage is controlled by maintaining tight operating clearances between the scrolls. This is accomplished by using an axially and radially compliant design in which the scroll wall tips make contact with their mating scroll disk. As mentioned above, scroll machining tolerances will be tightly maintained at  $\pm 0.0003$  inches [ $8\ \mu\text{m}$ ] on all surfaces. This will allow an average gap of  $0.0003$  inches [ $8\ \mu\text{m}$ ], which is needed to keep leakage reasonable.
- Leakage is “caught” by the additional wrap in the scrolls, which allows some useful work to be extracted out of the leakage flow.
- Limited axial deflection of the scrolls disks is essential to help maintain small gaps and manage leakage. This is achieved by keeping the scroll disk diameter relatively small, and also by providing balance pressure loads on both scrolls. For the fixed scroll, the balance pressure load is provided by a circular pocket at the expander inlet. For the orbiting scroll, an annular pocket is used. The annular pocket is fed high pressure refrigerant from the center of the scroll through a small pressure equalization passage. An annular shape is used for the orbiting scroll to make room for the offset bearing, which takes power from the orbiting scroll.

Designs and CAD models for a few different power-output configurations of the scroll expander were developed. These include shaft-output, an integrated expander/generator, an integrated first-stage compressor with an expander, and integration with the main motor/compressor. While a shaft-output configuration would be useful for proof-of-concept testing, this arrangement would not likely be acceptable for service in a military ECU, because the leakage associated with the shaft seal would necessitate regular addition of refrigerant charge every 2 or 3 years. The basic scroll expander arrangement of the shaft-output design is adaptable to any of the possible configurations which could be considered for making use of the power output in an ECU.

Weight estimates of the different expander configurations based on the CAD models for the first three configurations are as follows.

- Shaft-output: 12 lb [5.5 kg]
- Hermetic expander/generator: 20 lb [9.1 kg]
- Hermetic expander/compressor stage: 28 lb [12.7 kg]
- Integration with main compressor: 5 to 7 lb [2.3 to 3.2 kg] added weight.

Crankshaft bearing loads for a shaft-output scroll expander have been calculated, and preliminary bearing selections have been made, assuming use of hydrodynamic oil film bearings. Figure 3 below shows the crankshaft and illustrates the loading.

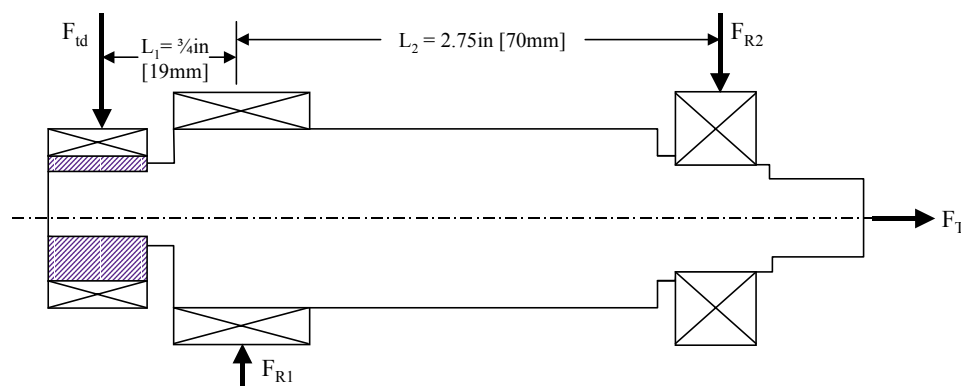


**Figure 3: Crankshaft Bearing Loads**

Based on a conservative estimate of 200 lb [890 N] for the tangential drive force  $F_{id}$ , the bearing forces and designs are summarized in Table 5 below. Analysis was done based on the Cast Bronze Bearing Design Manual (Rippel, 1979). Assumptions for the design are as follows.

- 3,500 rpm machine speed
- POE oil at 100 °F [38 °C] (viscosity of 10 centipoise)

The crankshaft bearing loads can certainly be supported with bearings of reasonable size, and the frictional losses associated with the bearings are small. If the scroll expander were integrated with a two-stage rotary compressor, the crankshaft bearings of the compressor serve as the crankshaft bearings for the expander. By orienting the eccentricity of the lower compressor stage 180° from the eccentricity of the scroll expander, loads on the compressor crankshaft bearings will be reduced.

**Table 5: Crankshaft Bearing Design Summary---Hydrodynamic Bearings**

	<b>Eccentric Bearing</b>	<b>Inboard Crankshaft Bearing</b>	<b>Outboard Crankshaft Bearing</b>
Load (lb [N])	200 [893]	275 [1,230]	75 [335]
Bearing Diameter (inch [mm])	0.75 [19]	1.00 [25]	0.625 [16]
Length (inch [mm])	0.5 [13]	0.75 [19]	0.5 [13]
Diametral Clearance (inch [μm])	0.0008 [20]	0.001 [25]	0.001 [25]
Minimum Gap (microinch [μm])	100 [2.5]	175 [4.4]	150 [3.8]
Friction Loss (hp [kW])	0.02 [.015]	0.05 [0.037]	0.01 [0.007]

Leakage of refrigerant through the scroll expander represents lost potential for energy recovery. As mentioned above, the design allows capture of some of the leaking refrigerant in downstream scroll pockets, where some useful work can still be extracted from the leakage flow. However, minimizing leakage will be of great importance in attaining desired efficiency levels.

CFD analysis was done to estimate the leakage to be expected for the anticipated scroll expander design. In particular, the tip leakage at the inlet of the expander was estimated. Key modeling parameters for this analysis are as follows.

- Gap dimensions 0.0003" [8 μm] high by 0.2" [5 mm] long.
- Applicable tip length is about 4 inches [102 mm].
- Inner pocket pressure of 2,000 psia [138 bar], outer pocket pressure of 1,000 psia [69 bar].
- Fluid remains supercritical.
- Fluid models used: Ideal gas, Liquid, Real Gas. The real gas model used a property data correlation based on literature data for supercritical CO<sub>2</sub> (Hauck and Weidner, 2000).

The flow is turbulent with Reynolds number above 5000. Tip leakage flow was calculated to be as follows for the ideal gas and liquid fluid models.

- Ideal Gas: 0.105 kg/m/s, or 84lb/hr [38 kg/hr] for the 4-inch [102 mm] gap.
- Liquid: 0.201 kg/m/s, or 162lb/hr [74 kg/hr] for the 4-inch [102 mm] gap.

The real fluid behavior is expected to be somewhere between the ideal gas and liquid models in terms of compressibility. Flank leakage should add roughly 10% to this leakage flow, since the leakage line length for the flank gap is about one-tenth that of the tip gap. Hence, a conservative estimate of the leakage is 150lb/hr [68 kg/hr]. This leakage flow represents about 20% of the system design flow. The CFD analysis does not take into consideration the potentially mitigating effect of refrigerant flashing as it enters the two-phase region while passing through the gap or the effect of oil. The analysis shows that expander volumetric efficiency will be acceptable.

Finite Element Analysis (FEA) was done to determine the stress levels and deflections of the scroll disk. The analysis addressed the deflection issue of most concern for the performance of the scroll expander, i.e. the possibility that the pressure loading would cause axial deflection of the scroll wall at the center of the scroll disk. Such a deflection could potentially open the tip gap sufficiently to significantly increase the leakage flow and make the device impractical.

The maximum stresses calculated for the orbiting scroll disk are about 6,500 psi [45 Mpa], well within stress limits of any material which would be considered for the scrolls. The tip deflections are on the order of 0.0001" [2.5 μm], which is not likely to result in significant additional tip leakage, further enhancing confidence that the scrolls can be made sufficiently stiff without making them extremely thick and heavy.

### Efficiency Projection

An estimate of the efficiency of the scroll expander has been made based on the preliminary design. Estimates of frictional losses are tabulated in Table 6 below. These estimates are based on the hydrodynamic oil film bearings which are consistent with a production expander. The efficiency of the expander is calculated as follows.

$$\text{Efficiency} = \left( \frac{\dot{m}_{ideal}}{\dot{m}_{actual}} \right) \left( \frac{\text{Actual pv work} - \text{friction losses}}{\text{Ideal pv work}} \right) = \left( \frac{1}{1.2} \right) \left( \frac{1.53 - 0.2}{1.53} \right) = 72\% \quad (1)$$

This efficiency level of 72% is significantly higher than the 60% assumption used in the cycle analysis, and suggests that the benefits of the expander may be greater than initially estimated.

**Table 6: Expander Friction Losses**

Surface	Friction Loss (hp [kW])
Crankshaft Bearings (Outboard and Inboard)	0.06 [0.045]
Eccentric Bearing	0.02 [0.015]
Axial Contact/Shear Friction	0.05 [0.037]
Axial Balance Pressure Seals	0.01 [0.007]
Flank Contact Friction	0.03 [0.022]
Oldham Coupling	0.02 [0.015]
<b>TOTAL</b>	<b>20 [0.15]</b>

## 4. SYSTEM INTEGRATION

Four approaches for utilization of expander shaft power were considered, as discussed above. Table 7 below provides a comparison of key design attributes of these approaches. Notes regarding assumptions and clarification of calculations is presented below.

**COP:** Percent changes are presented as compared with a system without an expander, for which overall COP is 1.21 (36,000Btu/hr [10.5 kW] capacity vs. 8.7kW input power). A conservative estimate of 60% is used for expander efficiency. Using an expander instead of the evaporator blower motor does not allow full use of the expander output power. However, the motor losses are also taken out of the evaporator side, thus reducing losses and increasing capacity. Motor efficiencies are assumed to be 90% for the compressor/expander and 86% for blower motors. For the generator option, both compressor motor and generator losses are added to power input (generator efficiency of 86% is assumed).

**Table 7: Key Design Attributes for Different Expander Configurations**

	Shaft-Output to Blower	Hermetic Expander/Generator	Hermetic Expander/First Stage Compressor	Hermetic Expander/Compressor
COP Increase of Expander	+19%	+19%	+23%	+23%
Net Weight Impact (lb [kg])	-13 [-5.9]	+15 [+6.8]	+18 [+8.2]	-2 [-0.9]
Size (inches [mm])	6φ x 8 [152φ x 203]	6φ x 10 [152φ x 254]	6φ x 12 [152φ x 305]	Compressor Height increase of 2 to 3 [50 to 75]
System Control Impact	Air flow impacted by available power output.	Control possible with variable speed generator	Slow system startup, little control	Constant expander speed

**Net Weight Impact:** Gross component weights are adjusted by weight differences for affected components, in particular for motors. A 36,000 Btu/hr [10.5 kW] ECU system without an expander is the baseline. The motor of a compressor serving such a system is assumed to have a 35 lb [16 kg] weight and 9.2 hp [6.9 kW]. Motor weights for the other systems are calculated assuming that motors are sized for the required loads and that they have the same weight per power ratio as the baseline motor. The evaporator blower motor is assumed to weigh 20lb [9.1 kg]. Weight savings of the compressor elements themselves (i.e. cylinders and pistons) are assumed negligible. Weight for the gas cooler is assumed to be proportional to gas cooler load, with is reduced 7% in an expander system.



Based on important criteria such as COP impact, weight, size and packaging, the integration with a compressor appears to be the most attractive option. Integration with the evaporator blower would potentially be attractive based on weight. However, performance issues associated with the blower's inability to utilize all of the expander output power and the fact that insufficient blower power will be available during off-design conditions combined with the added service associated with the open shaft make the evaporator blower approach less attractive. The generator approach is attractive because it is self contained, can be located anywhere within a system, and could be controlled to provide mass flow control. However, the added weight of this components makes it less attractive. Weight and complexity are also key drawbacks to integration with a first-stage compressor.

## 5. CONCLUSIONS

A design concept for a scroll expander to be used for improving the performance of CO<sub>2</sub>-refrigerant cooling systems has been developed. The work indicates that the proposed design is manufacturable using conventional manufacturing processes, is projected to operate at high efficiency levels, and will result in significant performance improvement for ECU's and air-conditioners which use CO<sub>2</sub> refrigerant. Key results of the work are as follows.

- Leakage losses are estimated to be approximately 20% for an expander serving a 36,000 Btu/hr [10.5 kW] military ECU.
- Scroll disk stresses are low at less than 10,000 psi [69 Mpa], well within the stress limits of any material which would be considered for the scrolls.
- Scroll disk axial deflections are low at about 0.0001 inch [2.5μm], due to the planned axial balancing approach.
- Friction losses represent a relatively small portion of the p-v work (about 15%).
- Our estimates of the overall efficiency of the expander is 72%.
- The system impact of the expander for a 36kBtu/hr [10.5 kW] ECU will be to reduce input power about 1.5 to 2kW, a reduction of close to 20% of the power input of a CO<sub>2</sub> system without an expander.
- Overall air-conditioning system weight increase associated with integration of the expander in a CO<sub>2</sub> system is expected to be small. There may in fact be a net weight reduction.
- CO<sub>2</sub> system performance with an expander will not be improved by the incorporation of a Suction Line Heat Exchanger (SLHX).

## NOMENCLATURE

CAD	Computer-Aided Drafting	CO <sub>2</sub>	Carbon Dioxide
COP	Coefficient of Performance	ECU	Environmental Control Unit
SLHX	Suction Line Heat Exchanger		

## REFERENCES

- [1] R. Heidelck and H. Kruse, 2000, Expansion Machines for Carbon Dioxide Based on Modified Reciprocating Machines, *Proceedings of the 4<sup>th</sup> IIR-Gustav Lorentzen Conference on Natural Working Fluids at Purdue*, West Lafayette, Indiana, USA, pp. 455-462
- [2] Robinson, D. and Groll, E., 1998, Efficiencies of Transcritical CO<sub>2</sub> Cycles with and without an Expansion Turbine, *International Journal of Refrigeration*, Vol. 21, No. 7, pp. 577-589.
- [3] Military Specification, Air Conditioners: Vertical and Horizontal, Compact, MIL-A-52767D, 2/8/1989
- [4] Purchase Description, Air Conditioner, Horizontal and Vertical, Compact, PD 4120-0121, 6/8/2001
- [5] Rippel, H.C., 1979, "Cast Bronze Bearing Design Manual", Cast Bronze Bearing Institute, Inc., September.
- [6] Hauck, A., and E. Weidner, 2000, "Thermodynamic and Fluid-Dynamic Properties of Carbon Dioxide with Different Lubricants in Cooling Circuits for Automobile Application", *Ind. Eng. Chem. Res.* 39, p. 4646.
- [7] TIAX LLC, 2003, "Refrigerant Expansion Energy Recovery System: Phase I SBIR Final Report", prepared for the U.S. Army, August 15.

## ACKNOWLEDGEMENTS

This work was supported with U.S. Army Phase I SBIR funding under Contract DAAB15-03-C-0001.